ROBOTIC FREE-ORIENTED ADDITIVE MANUFACTURING TECHNIQUE FOR THERMOPLASTIC LATTICE AND CELLULAR STRUCTURES

MANUEL LADRON DE GUEVARA[1], LUIS BORUNDA[2],
JEREMY FICCA[3], DARAGH BYRNE[4] and
RAMESH KRISHNAMURTI[5]
[1,3,4,5]*Carnegie Mellon University*
[1,4,5]*{manuelr|daraghb|ramesh}@andrew.cmu.edu* [3]*jficca@cmu.edu*
[2]*Universidad Politecnica de Madrid*
[2]*lborunda.eco@etsav.cat*

Abstract. This paper presents a novel Additive Manufacturing application of situated Robotic Fused Deposition Modeling (RFDM) for thermoplastic cellular and lattice structures, called Free-Oriented Additive Manufacturing (FOAM), to accommodate variations in spatial conditions, deposition direction, and geometry in order to adapt to complex infrastructure settings, thus, breaking the conventional layer-by-layer stacking principle and the constant constraint of locking the tip of the nozzle to the negative Z direction when fabricating at an architectural scale.

Keywords. Robotic 3D Printing; Situated Fused Deposition; Thermoplastic Lattice Structures.

1. Introduction

Fused Deposition Modelling (FDM) is the most common method of Additive Manufacturing (AM) or 3D printing to alter manufacturing processes, because it affords freedom of design, waste minimization, complex modelling and fast prototyping (Ngo et al. 2018). Both in practice and academia, AM techniques contribute to discovering new design methodologies coordinated to fit with emerging robotic fabrication techniques (Oxman R. 2008, Willmann et al. 2013).

Fabrication of architectural elements by robotic systems has been broadly reviewed (Warszawski 1984, Haas et al. 1995) foreseeing robotic ubiquity, advances in automation construction, deconstruction and re-customization, providing tools for reconsidering existing construction practices (Bock 2015). Large-scale AM requires data, which can be efficiently introduced into the informed design for improved functionality (Ackoff 1974), reproduced with uncanny precision by automated systems (Hack et al. 2014) and improve the economics of production even for highly complex geometries (de Soto et al. 2018).

Conventional FDM techniques follow a stacked, layer upon layer, continuous thermoplastic polymer deposition of material, which pose problems for large scale

Intelligent & Informed, Proceedings of the 24th International Conference of the Association for Computer-Aided Architectural Design Research in Asia (CAADRIA) 2019, Volume 2, 333-342.

prototyping and construction field application. Recent studies have explored adjustments to 3D printers and robotic arms, as well as developing highly specialized end effector tools for specific applications (Felbrich et al. 2018, Kwon et al. 2019), that considers thicker material, optimized tool-paths to avoid material waste, costs, and time-consuming processes.

Spatial FDM is a method by which molten polymer sections are configured in a space frame pattern, which has demonstrated capability of fabricating functional products with optimized performance (Liu et al. 2018), and reduce fabrication time for prototype prints by differentiating the local value of a printed specimen along the extrusion process (Mueller et al. 2014).

Robotic arms augment the scale of fabrication. Their benefits and application within design processes have been explored (Tam & Mueller 2017, Yuan et al. 2016). In particular, Branch Technology implements a RFDM technique slightly tilting the nozzle when required, and without changing the orientation of the base. Recent advances in robotic AM (Huang et al. 2018) explore near impossibility of in-situ printing unless the piece is anchored to the ground, and the need to generalize to novel design methodologies.

This paper describes an AM technique, which breaks the constraint of printing along a negative Z axis (Figure 1), and utilizes the compacity of the end effector tool, for maximum reach and robotic motion in order to print complex infrastructures. This technique requires the study of the physical tool, material, and specifically contextualized computational design and tool-path workflows.

This research also provides insight into possible applications of extending AM techniques using commercially available equipment. In particular, we implement a flexible printing orientation method, suitable for novel spatial FDM applications, where minimum equipment dimensions for maximizing geometric production capabilities is required.

Figure 1. Free-Oriented Additive Manufacturing printing in the +Z direction.

2. FOAM Technique

We describe a technique, Free-Oriented Additive Manufacturing (FOAM), for robotic printing on an existing infrastructure, which bypasses assembly of parts, and decreases both cost of and time for construction. FOAM is able to cooperate with gravity and print in a counter-intuitive fashion. We explore variability by being able to change orientation of the tool while printing, by not constraining the tip of the nozzle to pointing down. We consider application to non-planar, curved infrastructures, and contrast this approach with conventional techniques.

2.1. EXTRUSION SYSTEM

2.1.1. End of the Arm Tool (EOAT)

To achieve maximal freedom of orientation and maneuverability, a compact unit is designed with all needed components for printing, integrated at the EOAT. The extrusion system is housed in a small box as illustrated in Figure 2, containing the motherboard and electronic components, a material spool as a feeder source, and a commercial extruder. The distance between the default Tool Center Point (TCP) and the tip of the nozzle is 450mm, perpendicular to the normal vector of the ATI plate. Collision cushioning is achieved by elongating the distance between the nozzle and the electronic box with a non-rigid 50x300x3mm aluminum plate, making it flexible enough to bend under collision, protecting the nozzle from breaking. For simplicity, no scanning tools or proximity sensors were employed.

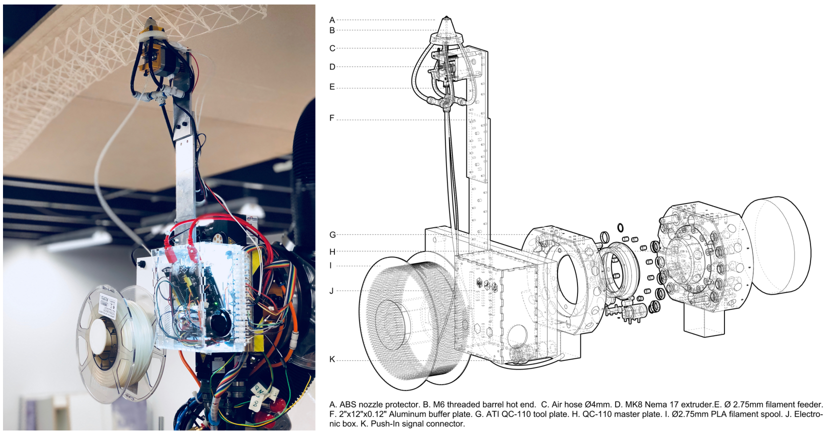

Figure 2. FOAM tool components: (Left) The working tool mounted on the robot arm. (Right) An annotated view of the components .

2.1.2. Thermoplastic Polymer Extrusion System

To make a cost-effective tool, we harvested components from commercial 3D printers. A regular 1.75mm diameter MK8 extruder is adapted for an M6 threaded barrel to feed a 3mm diameter thermoplastic filament through its interior. The barrel is wrapped with a 22 gauge nichrome wire, 1.04m length, yielding a resistance of 3.5 ohms to provide 12VDC 60W. This is sufficient to keep the nozzle at a melting temperature, up to 300C, within the range of the types of thermoplastics tested (PLA, PLA+, ABS, PETG). A 0.33mm stainless-steel wire was also tested, using 1.5m length of wire to obtain the same resistance. An NTC 3950 100K Thermistor as temperature sensor is attached to the tip of the barrel. To protect the hot-end from the ambient temperature, ceramic-fiber insulation and an ABS printed cover are needed. This custom piece also holds four air-hoses connected to the 6640 ABB air supply unit, solidifying the material upon extrusion. Best results are obtained by keeping a distance of 25 - 40mm between the air hose and the tip of the nozzle, maintaining an operating air pressure of 15 PSI. An electronic box contains Arduino boards to control temperature and feed flowrate. The logic voltage of the A4988 motor driver varies from 3 to 5.5v, having a max current per phase of 2A if pressurized cooling air is provided, or 1A otherwise.

2.1.3. Printing Materials

FOAM uses commercial 3mm diameter filament rolls which can result in 4mm thick printed material, depending on time, feed-rate and velocity parameters. For instance, if velocity of the robot is set to 3mm/s, and feed rate is set to 1/8 steps/s , it would generate ˜3.5mm extrusion. Maintaining the same feed-rate and incrementing the speed of the robotic arm to 8mm/s, reduces thickness to 20%.

Tested thermoplastic filament rolls include PLA, PLA-PRO, ABS and PETG. ABS and PETG offer higher capabilities than PLA such as lightweight properties (1.04, 1.23 and 1.24g/cm3 respectively), major elongation at break (22%, 228% and 8%), and major distortion temperature. Although not vitrifying as quickly as ABS or higher temperature thermoplastics, PLA presents the best results as it maintains a successful melting point at a wider temperature range, 190 - 210 (see Table 1.).

Table 1. Thermoplastic properties, eSUN Industrial CO.LTD.

FILAMENT	Print Temp(°C)	Density (g/cm3)	Distortion Temp (°C, 0.45MPa)	Melt Flow Index (g/10min)	Tensile Strength (MPa)	Elongation at Break (%)	Bending Strength (Mpa)
PLA	190 – 210	1.24	56	5(190°C/2.16kg)	65	8	97
PLA+	205 – 225	1.24	52	2(190°C/2.16kg)	60	29	87
ABS	220 – 270	1.04	78	12(220°C/10kg)	43	22	66
ABS+	220 – 270	1.06	73	15(220°C/10kg)	40	30	68
PETG	230 – 250	1.23	64	20(250°C/2.16kg)	49	228	68

2.1.4. Robotic Reach

To print freely in the space, it is possible to mount a pellet feeding system on the robotic arm, locking the nozzle position in its -Z direction (Soler et al. 2017). Alternatively, configurations can be liberated from the axis constraint by developing a highly engineered system to achieve a steady supply of plastic pellets, compromising cost-effectiveness (Oxman N et al. 2013). To expand the reach of the robotic arm and reduce system cost, we work closely with a commercial 3D printer configuration, housing its components and feeding system directly at the

EOAT, thus, being able to print over non-horizontal and non-planar infrastructures at reduced cost (see Figure 3.).

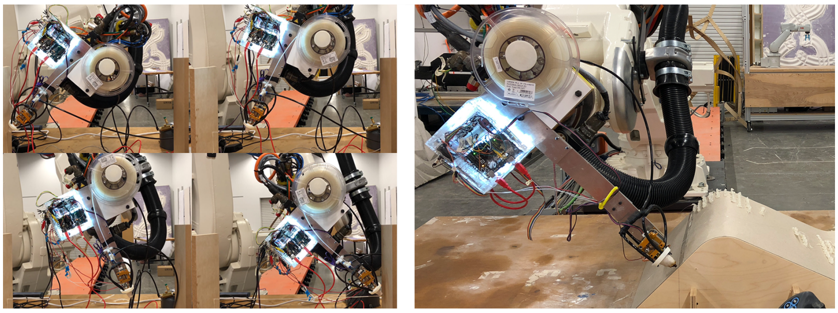

Figure 3. (Left) Tool operating within a 80cm space between vertical walls. (Right) FOAM applied over a non-planar surface.

2.2. FREE ORIENTED ADDITIVE MANUFACTURING METHOD

2.2.1. PID, Cooling System, and Stepper Synchronization

A critical factor for consistent filament extrusion is the control of temperature. For this, we use a proportional integral-derivative (PID) algorithm, a standard for industrial control systems.

2.2.2. Physical Constraints

The process starts by heating up the nozzle at a melting temperature. The robotic arm moves the hot end following a given toolpath. Normally rectilinear segments are chosen over a curvilinear typology, as the latter would require alternative techniques to solidify the material in such shape. Each point of discontinuity has a different wait time, to ensure proper solidification of the molten plastic and accurate bonding with already printed material. The algorithm is capable of computing a print at any orientation and direction without altering the quality of the print, challenging the force of gravity in the process. The direction and taper of angles are directly constrained by the angle of the nozzle (Figure 4a).

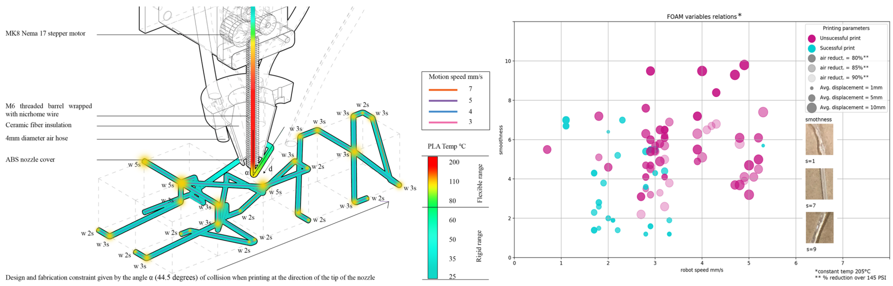

Figure 4. a. (Left) Spatial printing analysis. b (Right) Printed tests varying FOAM parameters.

3. Computational Methods

3.1. DESIGN

Two distinct algorithms were tested to design the workpieces of each case study.

The first is a similar to an oct-tree algorithm, for cellular structures, which determines whether a voxel lies inside or outside the volume. We assign a set of polylines to each voxel, which respond to a design criteria. The algorithm computes an overall set of individual geometries, responding to parameters such as opacity, structural behavior and material budget. The principal part of the algorithm ensures that every unit is printable and that none collide with the already printed neighbor. A backtracking algorithm finds a printable in-budget solution, making the design process informed by its inherent physical and material fabrication constraints.

The second creates two NURBS surfaces from two distinct pairs of splines, extracting a lattice structure based on repetitions of the following pattern: short supporting segment, diagonal downward segment, short supporting segment and diagonal upward segment. We consider the curvature contrast between surfaces, one maintaining curvature in the U direction, and the other in the V direction. The potential error in fabrication presented by curvature differences is balanced by an algorithm that weaves the lattices connecting their nodes (Figure 5).

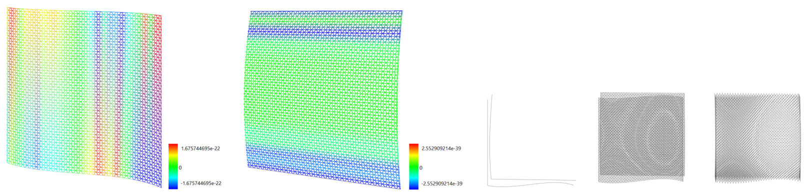

Figure 5. Design Process for Lattice Structures.

3.2. FABRICATION

A tectonic approach that considers affordances and limitations of material, and the physical tool is recommended. However, anticipating constraints does not ensure clean and fail-safe fabrication. The main challenge is that the nozzle has to respect material already printed in order to prevent collisions. For instance, in the cellular structure algorithm, collision detection between voxels is checked. To overcome unforeseen problems, a feedback loop between the design and fabrication processes is implemented. For efficiency, an offset in the Z direction higher than the voxel's height is applied to the first and last points of the polyline at each cell. This ensures that the nozzle never collides with already printed geometries during non-printing motions.

4. Case Studies

Two case studies have been tested to accommodate both structures. The cellular structure is tested by conventional 3D spatial printing, locking the nozzle at the negative Z axis; the lattice structure is tested at different orientations using two configurations: implementing a dynamic multi-robot workflow, and printing over a 4m height ceiling, locking the nozzle at the positive Z axis.

4.1. CELLULAR STRUCTURE

A volume is discretized into smaller units using a multi-resolution approach. The underlying 3D grid stores information such as material and geometry at each voxel. Testing a range of printable polylines from simple to complex give insights into the type of design nomenclature feasible for this fabrication technique.

Acute angles present a lower fidelity to the digital model than obtuse angles. Consecutive segments shorter than 10mm start to blur the overall appearance of the cell. Printing temperatures above 220C for PLA result into sagged segments. Otherwise, an excess of cool temperature, below 180C, yields rigid segments that produce undesirable low-fidelity outcomes. These constraints might be overcome by changing feed-rate flow, wait times and the motion of the robot; it is also necessary to find a contextualized balance between design limitations and time cost. The variability of the results compromise the clarity of the relation between parameters and geometrical path. However, the relation between the robotic arm speed and air pressure yields a clear distinction. An increase in speeds beyond 4mm/s requires design re-adjustment (see Figure 4b). It is important to note that material texture is less smooth when the PLA spool has higher humidity levels.

4.2. LATTICE STRUCTURE

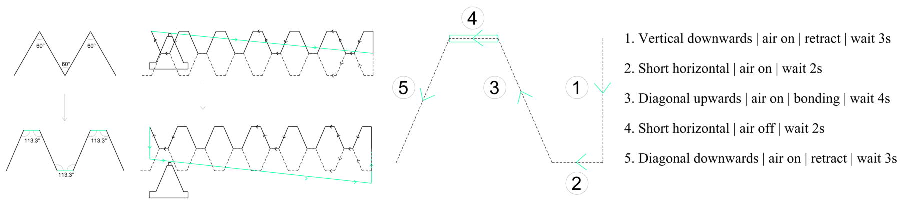

Figure 6. Physical constraint feedback into design process.

Lattice structures are generally organized by rows of repeated patterns. The results provided by the cell structure method informs the design of the pattern for the lattice structure. Consider a proper equilateral-triangular pattern. Although within a printable range, it presents drawbacks such as a lack of horizontal support for upper rows, as well as a risk of decrease in the height of the triangle, since acute angles are prone to bow towards the direction of printing due to the tensile strength carried by the nozzle. A workaround is to introduce small horizontal segments at the vertices, so that the acute 60° angles are converted to a 113° obtuse angle. To avoid collisions, this typology requires adding an offset point at the beginning and end of each row (Figure 6).

The material behavior was tested at a smaller scale by the use of two robotic arms synchronized so that an ABB IRB 4400 arm grips an MDF base at a given orientation. An ABB IRB 6640, which holds the printing tool, starts printing the lattice structure until the first robot changes the orientation and position of the board. The printing robot readjusts its position to continue printing from the last point printed at the previous position (Figure 7). This test provides two major breakthroughs:

- The algorithm adjusts the flowrate and applies a retraction force based on the orientation of the tool. This immediately nullifies gravitational forces in the print process.
- The same lattice structure has been tested over horizontal, vertical and other four different orientations. With the right parameters relative to each orientation, no difference in material quality nor geometry deformations are presented.

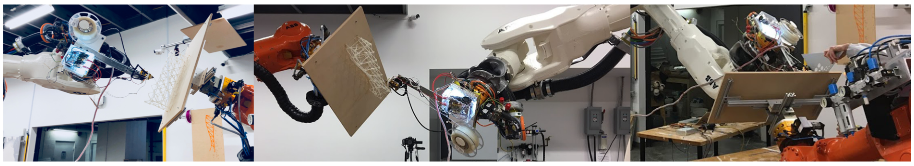

Figure 7. FOAM technique tested over a dynamic variable setting.

For the final case study we created a fully automated set-up using an ABB IRB 6640 arm, with a maximum reach of 2.55m and a wrist torque of 1324 Nm. The workpiece bounding box dimensions are 2x1x0.3m, fabricated as a single piece, having its base on an MDF board attached to a metallic beam structure on the ceiling at a 4.20m height. The robotic arm lies on a 6m track.

The lattice structure is divided into main patterned rows, a continuous cord that lies over each patterned row, and diagonals that connects the nodes of each side of the lattice. The robot is then actuated so it varies its motion velocity depending on these three parts and on the grammar of the pattern, following the instructions given in Figure 6.

The piece was completed in 40 hours, printing each patterned row in 18 minutes, each continuous cord in 8 minutes, and each weaving sequence in 35 minutes at its maximum dimension. Different wait times were implemented depending on geometry and context of the process; intermittent air unit was crucial in this process. This test demonstrates that the scalability problem of 3D printing can be overcome by printing in-situ a single piece, reducing logistic and assembly costs. Due to the lightweight nature of thermoplastic polymers, the FOAM technique can print large single structures that might support greater overhangs than other manufacturing processes.

5. Results and Discussion

This research used a 6-axis ABB robotic arm mounted on a 6m length track, which can reach any point within the robotic work-cell, with any given orientation, making the printing optimal for the adaptability to 3D print on complex geometric settings. The main authors have previously tested similar tool-path algorithms on normal horizontal settings, where the referenced parameters were tested built on top of other research works (Liu et al. 2018). In our tests, PLA proved to be a more successful print material as compared with ABS or PETG. One of the challenges for spatial printing is synchronizing robotic arm motion, stepper feed-rate, wait times and cooling system. Overall, a 3mm/s speed and 1/8 motor step has proven to yield successful filament thickness when printing horizontally. We have found that, accommodating these variables to the orientation of the piece, the printed structure maintains a 7% difference from its digital version in all tested orientations. Thus, gravity does not have a major effect on the deformation ratio.

Improvements to the design tool and fabrication algorithms resolve fabrication hurdles that are inherent to FDM. We acknowledge that despite using a relatively simple printing tool, a sophisticated computational control system is required to print using this technique, since it is the algorithms as outlined that contribute to FOAM's success and advancements over fundamental printing techniques.

There are still drawbacks present in the FOAM process:

- Time cost is still inefficient. This might be overcome by reducing wait times at each node and speeding up the robotic motion, however, more extensive research is required.
- Thermoplastic polymers, although lightweight and cost-effective, have deficient ecological footprint, and present a lack of tensile strength and durability for direct construction application. Correctly assessing anisotropic mechanical behavior in FDM is a general challenge. The incorporation of reinforced plastics or metals (Blonder & Grobman 2015, Kwon et al. 2019, Mitchell et al. 2018) is a step forward to applying FOAM to construction.
- There are limits to designs reflected by the limitations of the tool. The nozzle should be optimized to avoid collisions with already printed material. A thinner nozzle has a larger printable angle range than a thicker nozzle. We focusing on an improved tool with a thinner nozzle for printing with reinforced thermoplastic materials.

FOAM provides a novel fabrication technique for architectural applications in previously unexploited spaces, providing the means for reconfiguring and bonding new qualities to existing non-necessarily planar nor horizontal infrastructures. This entails a reduction in logistic and assembly costs. It also opens up possibilities for new design methodologies in practice and academic institutions. Using robots in pedagogical frames can speed up research in design, creating new aesthetic sensibilities that right now are difficult to assess due to the lack of precedents, as we are in the shift of using new science with old machines (Carpo 2017).

Acknowledgments

This research was supported by The Frank Ratchye Fund for Art @ the Frontier and Consejo Social de la Universidad Politécnica de Madrid (UPM). The authors would like to thank the advising team, Professors Josh Bard, Daniel Cardoso, and Mary-Lou Arscott from Carnegie Mellon University (CMU). Also, we would to thank Prof. Jesus Anaya from UPM, and the head of the school of architecture of CMU, Prof. Steve Lee, for making possible this international collaboration.

References

Ackoff, R.L.: 1974, Redesigning the future, *Proceedings of an IFORS Specialized Conference on Operational Research and the Social Sciences*, New York, 29.

Blonder, A. and Grobman, Y.J.: 2015, Design and fabrication with fibre-reinforced polymers in architecture: a case for complex geometry., *Architectural Science Review*, **59**, 257-268.

Bock, T.: 2015, The future of construction automation: Technological disruption and the upcoming ubiquity of robotics., *Automation in Constructiotn*, **59**, 113-121.

Carpo, M.: 2017, *The Second Digital Turn: Design Beyond Intelligence*, MIT Press.

Felbrich, B., Wulle, F., Allgaier, C., Menges, A. and Verl, A.: 2018, A novel rapid additive manufacturing concept for architectural composite shell construction inspired by the shell formation in land snails, *Bioinspiration & biomimetics*, **13**(2), 26010.

Jimenez Garcia, M., Retsin, G. and Soler, V.: 2017, A Generalized Approach to Non- Layered Fused Filament Fabrication, *ACADIA 2017*, 562-571.

Haas, C., Skibniewski, M. and Budny, E.: 1995, Robotics in civil enegineering, *Microcomputers in Civil Engineering*, **10**, 371-381.

Hack, N.H., Lauer, W.V.L., Gramazio, F.G. and Kohler, M.K.: 2014, Mesh Mould: Differentiation for Enhanced Performance, *Proceedings of CAADRIA 2014*, Hong Kong, 139-148.

Huang, Y., Carstensen, J., Tessmer, L. and Mueller, C.: 2018, Robotic Extrusion of Architectural Structures with Nonstandard Topology, *ROBARCH 2018*, Zurich, 377-389.

Kwon, H., Eichenhofer, M., Kyttas, T. and Dillenburger, B.: 2018, Digital Composites: Robotic 3D Printing of Continuous Carbon Fiber-Reinforced Plastics for Functionally-Graded Building Components, *Robotic Fabrication in Architecture, Art and Design*, 363-376.

Liu, S., Li, Y. and Li, N.: 2018, A novel free-hanging 3D printing method for continuous carbon fiber reinforced thermoplastic lattice truss core structures, *Materials and Design*, **137**, 235-244.

Mitchell, A., Lafont, U., Holynska, M. and Semprimoschnig, C.: 2018, Additive Manufacturing-A Review of 4D Printing and Future Applications, *Additive Manufacturing*, **24**, 606-626.

Mueller, S., Im, S., Gurevich, S., Teibrich, A., Pfisterer, L., Guimbretière, F. and Baudisch, P.: 2014, WirePrint: 3D Printed Previews for Fast Prototyping, *Proceedings of the 27th annual ACM symposium on User interface software and technology - UIST*, Honolulu, 273-280.

Ngo, T., Kashani, A., Imbalzano, G., Nguyen, K.T.G. and Hui, D.: 2018, Additive manufacturing (3D printing): A review of materials, methods, applications and challenges, *Composites Part B: Engineering*, **143**, 172-196.

Oxman, R.: 2008, Digital architecture as a challenge for design pedagogy: theory, knowledge, models and medium, *Design Studies*, **29**, 99-120.

Oxman, N., Laucks, J., Kayser, M., Tsai, E. and Firstenberg, E.: 2013, Freeform 3D printing: Towards a Sustainable Approach to Additive Manufacturing, *Green Design, Materials and Manufacturing Processes*, **479**, 479-483.

Garcia de Soto, B.G., Agustí-Juan, I., Hunhevicz, J., Graser, K., Habert, G. and Adey, B.T.: 2018, Productivity of digital fabrication in construction: Cost and time analysis of a robotically built wall, *Automation in Constructiotn*, **92**, 297-311.

Tam, K. and Mueller, C.: 2017, Additive Manufacturing Along Principal Stress Lines, *3D Printing and Additive Manufacturing*, **4**, 63-81.

Warszawski, A.: 1984, Application of Robotics to Building Construction, *Proceedings of the 1st International Symposium on Automation and Robotics in Construction (ISARC)*.

Willmann, J., Gramazio, F., Kohler, M. and Langenberg, S.: 2013, Digital by Material, *Rob|Arch 2012*, Vienna, 12-27.

Yuan, J., Jianke, D., Yong, H. and Guiqiang, F.: 2017, Modeling and Process Planning for Curved Layer Fused Deposition, *The International Journal of Advanced Manufacturing*, **91**, 273-285.